J. Am. Soc. Mass Spectrom. (2013) 24:1997–2006
DOI: 10.1007/s13361-013-0729-3

RESEARCH ARTICLE

Gas-phase Dissociation of homo-DNA Oligonucleotides

Silvan R. Stucki, Camille Désiron, Adrien Nyakas, Simon Marti, Christian J. Leumann, Stefan Schürch

Department of Chemistry and Biochemistry, University of Bern, Bern, Switzerland

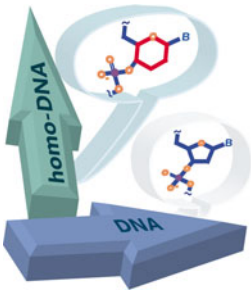

Abstract. Synthetic modified oligonucleotides are of interest for diagnostic and therapeutic applications, as their biological stability, pairing selectivity, and binding strength can be considerably increased by the incorporation of unnatural structural elements. Homo-DNA is an oligonucleotide homologue based on dideoxy-hexopyranosyl sugar moieties, which follows the Watson-Crick A-T and G-C base pairing system, but does not hybridize with complementary natural DNA and RNA. Homo-DNA has found application as a bioorthogonal element in templated chemistry applications. The gas-phase dissociation of homo-DNA has been investigated by ESI-MS/MS and MALDI-MS/MS, and mechanistic aspects of its gas-phase dissociation are discussed. Experiments revealed a charge state dependent preference for the loss of nucleobases, which are released either as neutrals or as anions. In contrast to DNA, nucleobase loss from homo-DNA was found to be decoupled from backbone cleavage, thus resulting in stable products. This renders an additional stage of ion activation necessary in order to generate sequence-defining fragment ions. Upon MS^3 of the primary base-loss ion, homo-DNA was found to exhibit unspecific backbone dissociation resulting in a balanced distribution of all fragment ion series.

Key words: Gas-phase fragmentation, Modified nucleic acids, homo-DNA, Nucleobase loss, Sugar-modification, ESI-MS, MALDI-MS, Bioorthogonality

Received: 14 May 2013/Revised: 2 August 2013/Accepted: 7 August 2013/Published online: 17 September 2013

Introduction

Short synthetic oligonucleotides, which interact with natural nucleic acids, have gained increased attention as diagnostic tools for DNA or RNA recognition. Within the past decades, a variety of highly modified oligonucleotide analogues exhibiting improved biological stability and base-pairing properties has been developed. Numerous modifications of the phosphate backbone, the sugar moiety, and the nucleobases have been evaluated for their effectiveness to enhance the properties of synthetic oligonucleotides [1–5].

The oligonucleotide-templated reaction (OTR) approach is an effective tool to detect nucleic acids in vivo [6]. The key features of this method include two oligonucleotides that each contain a reactive group and are complementary to a specific template sequence in the target cell, on which they are hybridizing adjacently. Due to the spatial proximity of the reactive groups after hybridization, a chemical reaction is triggered, upon which, for example, a profluorophore is converted into a fluorophore. This technique allows for facile sensing of the hybridized oligonucleotide by means of fluorescence spectroscopy [7, 8]. A similar principle was applied by Erben et al. who reported a DNA template-triggered, sequence-specific transfer of an aminoacyl group from one phosphorothioate modified PNA-peptide hybrid to another [9]. The DNA template was even found to act catalytically by binding new probes after the modified peptidyl-PNA conjugate was released.

Another intriguing application of the DNA-template approach is oligonucleotide mediated drug release [10, 11]. Saito and coworkers used the molecular beacon approach, in which they implemented a photoactive phenacyl group with an attached drug to the template oligodeoxynucleotide. The probe oligodeoxynucleotide also contained a naphthalene group, causing triplet quenching of the phenacyl group and, consequently, stabilization of the drug–phenacyl bond when the stem-loop structure was adopted [11]. Upon hybridization with the target sequence, though, the template oligonucleotide assumed an open form, in which the triplet quencher lost its influence and, thus, drug release by irradiation at 312 nm was facilitated. In a recent study,

Electronic supplementary material The online version of this article (doi:10.1007/s13361-013-0729-3) contains supplementary material, which is available to authorized users.

Correspondence to: Stefan Schürch; *e-mail:* stefan.schuerch@ioc.unibe.ch

Stoop et al. demonstrated an OTR using a molecular beacon consisting of a hybrid homo-DNA/DNA oligonucleotide for the recognition of single-stranded DNA and RNA [12]. The chimeric probe consists of a hybridizing DNA sequence, which is responsible for selective binding to a complementary single-strand, and a bioorthogonal homo-DNA linker, which either carries the profluorophore or the activator [12]. Upon hybridization with the target sequence, the profluorophore is converted into the active fluorophore, thus reporting the presence of the target. Incorporation of the homo-DNA linker sequence results in spatial and functional decoupling of the sensing DNA from the reporting system, thus offering the opportunity for individual optimization of each system's performance.

Homo-DNA is a DNA analogue that consists of 2',3'-dideoxy-β-D-glucopyranosyl nucleotide linker (Scheme 1) [13–15]. The hexopyranosyl sugar moieties are interconnected in a 4'-6' manner to form oligonucleotides. Homo-DNA is able to build anti-parallel duplexes via Watson-Crick base pairing. Additionally, pairing of two purines (G-G, A-A) can be accomplished by reversed Hoogsteen hydrogen bonding. Due to the high degree of irregular rise and twist properties and the greater internucleotide distance, homo-DNA does not hybridize with complementary DNA and RNA sequences.

Homo-DNA oligomers were originally synthesized by Eschenmoser and co-workers with the goal to understand why nature has chosen pentoses over hexoses for building up the genetic code [13]. Besides the ambition to answer such a fundamental question, homo-DNA has gained interest as a bioorthogonal linker element for templated chemistry applications, such as synthesis of chemical libraries or nucleic acid sensing and imaging [16–18].

Due to the ineffectiveness of classical sequencing techniques for the characterization of relatively short unnatural oligonucleotides, tandem mass spectrometry has become the method of choice for their sequence determination and detailed structural investigation. Based on the work of several research groups, extensive knowledge about the gas-phase behavior of natural [19–24] and modified oligonucleotides [25–29] has been acquired over the past two decades and in many cases tandem mass spectrometric sequencing has become routine.

However, if so far unexplored structural elements are present in a synthetic oligonucleotide, which directly affect its backbone dissociation and, thus, the generation of sequence-defining fragment ions, fundamental studies are needed to provide the basis for future tandem mass spectrometric investigations. Herein, we report on the gas-phase dissociation of homo-DNA by collisional activation. Experiments were carried out by electrospray ionization tandem mass spectrometry (ESI-MS/MS) on a linear ion trap/Orbitrap instrument, and by matrix-assisted laser desorption/ionization time-of-flight tandem mass spectrometry (MALDI-MS/MS). The main dissociation products are identified and fragmentation pathways are discussed.

Experimental

Oligonucleotides, Chemicals, and Solvents

The single-stranded 21-mer oligodeoxynucleotide was custom-synthesized by Trilink Biotechnologies (San Diego, CA, USA) as ammonium salt. Oligonucleotide stock solutions were prepared by dissolving the lyophilized material in water to a concentration of 1 nmol/μL. For analysis in the negative ion mode, the stock solutions were diluted with 1:1 methanol/water to yield an oligonucleotide concentration of 25 pmol/μL. For analysis in the positive ion mode the oligonucleotide concentration was 50 pmol/μL in 1:1 methanol/water containing 2 % vol. formic acid. All matrix compounds and HPLC-grade solvents were purchased from Sigma-Aldrich (Buchs, Switzerland). Homo-DNA oligonucleotides were synthesized according to the previously published procedure [30].

Electrospray Ionization Mass Spectrometry (ESI-MS)

ESI-MS experiments were performed on a LTQ Orbitrap XL mass spectrometer (Thermo Fisher Scientific, Bremen, Germany), equipped with a nano-electrospray ion source. Experiments were carried out in the negative and positive ion mode. Potentials applied to the nano-electrospray needle were between –850 V and –1000 V in the negative ion mode

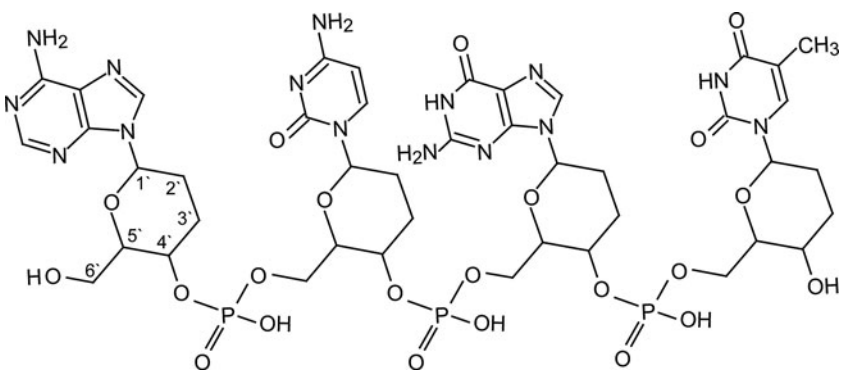

Scheme 1. Structure of a homo-DNA tetramer with the nucleotides linked in a 4'-6'-fashion

and between 1200 V and 1400 V in the positive ion mode. Mass spectra were acquired in the FTMS mode from *m/z* 100 to *m/z* 2000 with the mass resolution set to 100,000 (m/Δm at *m/z* 400). The source conditions were as follows: capillary temperature 200 °C, capillary voltage ± 50 V, tube lens voltage ± 218 V. For collision-induced dissociation in the linear ion trap, precursor ions were selected within a window of ± 3 *m/z* units and relative collision energies (rCE) in the range from 15 % to 40 % were applied. The activation time was 100 ms and helium was used as the collision gas. Higher-energy CID activation was carried out in the HCD cell of the instrument, with nitrogen as the collision gas and a rCE of 35 %. The Xcalibur Software Suite including Qualbrowser ver. 2.0.7 (Thermo Fisher Scientific) was used for data processing. Peak assignment was supported by the OMA & OPA software tool [31].

MALDI Mass Spectrometry

MALDI-TOF-MS experiments were carried out on an Autoflex III instrument (Bruker Daltonics, Bremen, Germany), equipped with a LIFT CID cell [32]. For experiments in the negative ion mode 2,4,6-trihydroxy acetophenone (18 mg/mL), dissolved in 1:1 acetonitrile/water, was used as the matrix. An aqueous solution of triammonium citrate (24 mg/mL) was used as co-matrix. Matrix and co-matrix solutions were mixed with the oligonucleotide solution in a 1:1:2 ratio directly on the MALDI plate. For experiments performed in the positive ion mode, α-cyano-hydroxycinnamic acid (5 mg/mL) in 1:1 acetonitrile/water containing 0.5 % vol. formic acid was used as the matrix. Matrix and sample solution were applied in a 1:1 ratio (1 μL of each) to the MALDI plate.

Results and Discussion

In order to elucidate the characteristics of the gas-phase dissociation of homo-DNA, the four sugar-modified oligonucleotides ***h1***–***h4*** and the DNA sequence ***d1*** (Table 1) were subjected to collision-induced dissociation in the linear ion trap and the product ions were monitored in the Orbitrap analyzer. Alternatively, activation of the precursor ions was achieved by higher-energy collision induced dissociation (HCD). Analyses were performed in the negative and positive ion mode. The resulting product ion spectra are compared and the effect of the substitution of the ribose by the hexopyranosyl moiety is discussed. Because the sequence ***h4*** was designed as a spacer element between a sensing DNA sequence and a fluorophore in templated chemistry experiments, it comprises an additional phosphate group and hexylamine linker at its 6'-end.

Collision-Induced Dissociation of homo-DNA Anions

Analysis of homo-DNA in the negative ion mode is preferred because of the facile deprotonation of the phosphate backbone.

Table 1. Sequences and Monoisotopic Masses of the Investigated Oligonucleotides. The Sequence h4 Carries an Additional Hexylamine Linker ($NH_2(CH_2)_6$) for Binding of a Fluorophore

Sequence	Length	Name	Mass
$(G_3T_3)_3GGG$	21-mer	h1	6917.481
(ACGTGC)	6-mer	h2	1875.440
(ATAGGC)	6-mer	h3	1899.451
$NH_2(CH_2)_6$-(GCCTA)	5-mer	h4	1711.443
$(G_3T_3)_3GGG$	21-mer	d1	6623.242

In addition to the peaks of multiply deprotonated homo-DNA, the spectra show peaks corresponding to duplex structures, thus giving evidence for the previously reported strong non-Watson-Crick self-paring tendency of homo-DNA (Supplemental Figure S1) [13]. Tandem mass spectrometric experiments revealed considerable differences between the dissociation of homo-DNA and the corresponding unmodified ribose-based DNA sequences. The product ion spectra of homo-DNA are characterized by strong signals attributable to the release of

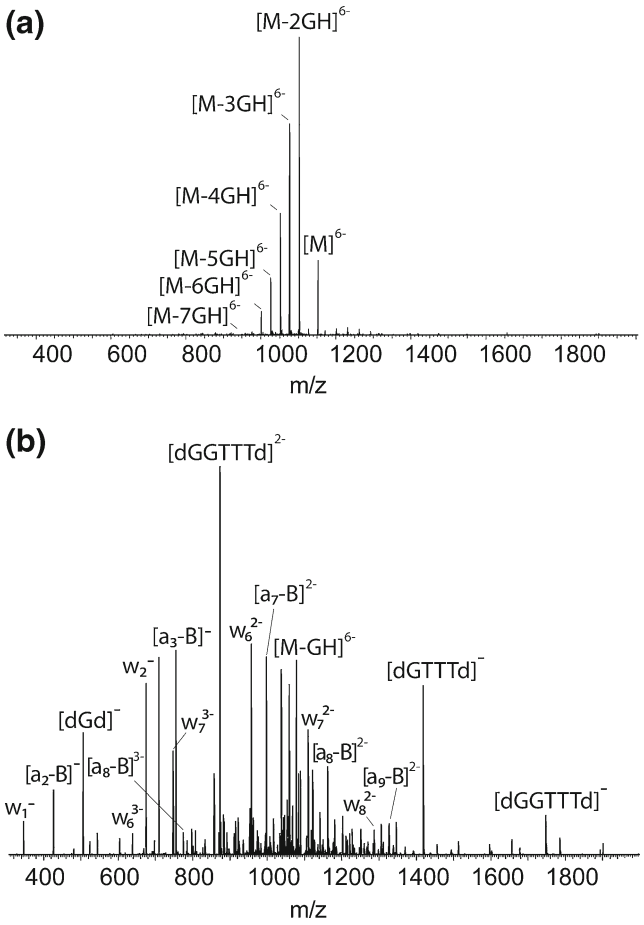

Figure 1. Ion trap product ion spectra of the 21-mer homo-DNA **h1 (a)** and the ribose-based DNA **d1 (b)** exhibiting the same nucleotide sequence. Six-fold deprotonated oligonucleotides were selected for CID. Both mass spectra were obtained with identical activation parameters (rCE=40 %, 100 ms activation time)

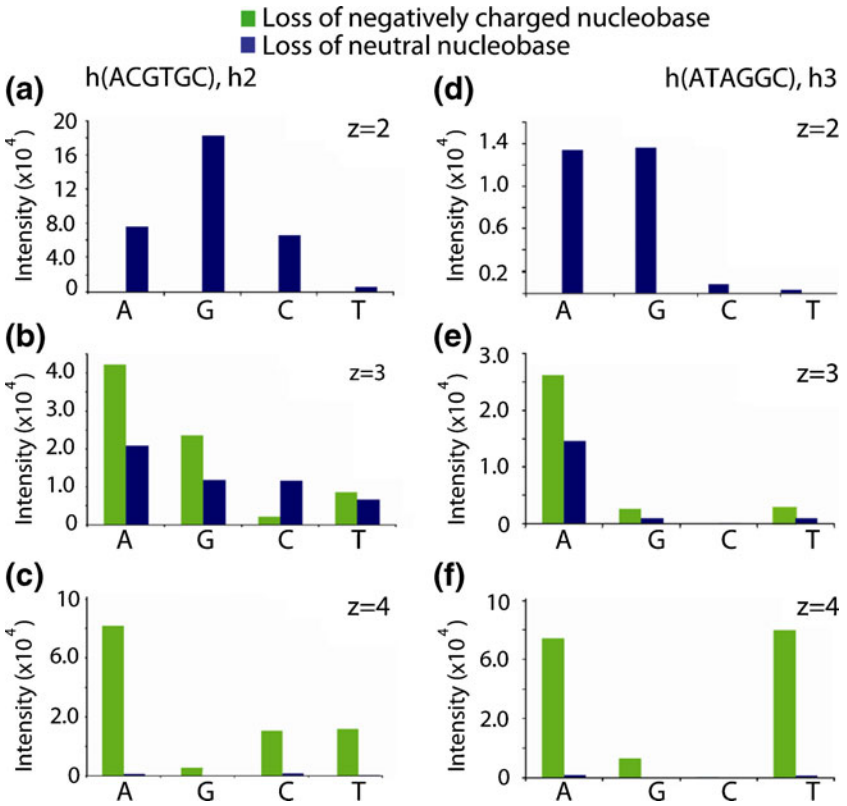

Figure 2. Charge state dependent loss of neutral and negatively charged nucleobases from the deprotonated homo-DNA sequences **h2** (left) and **h3** (right)

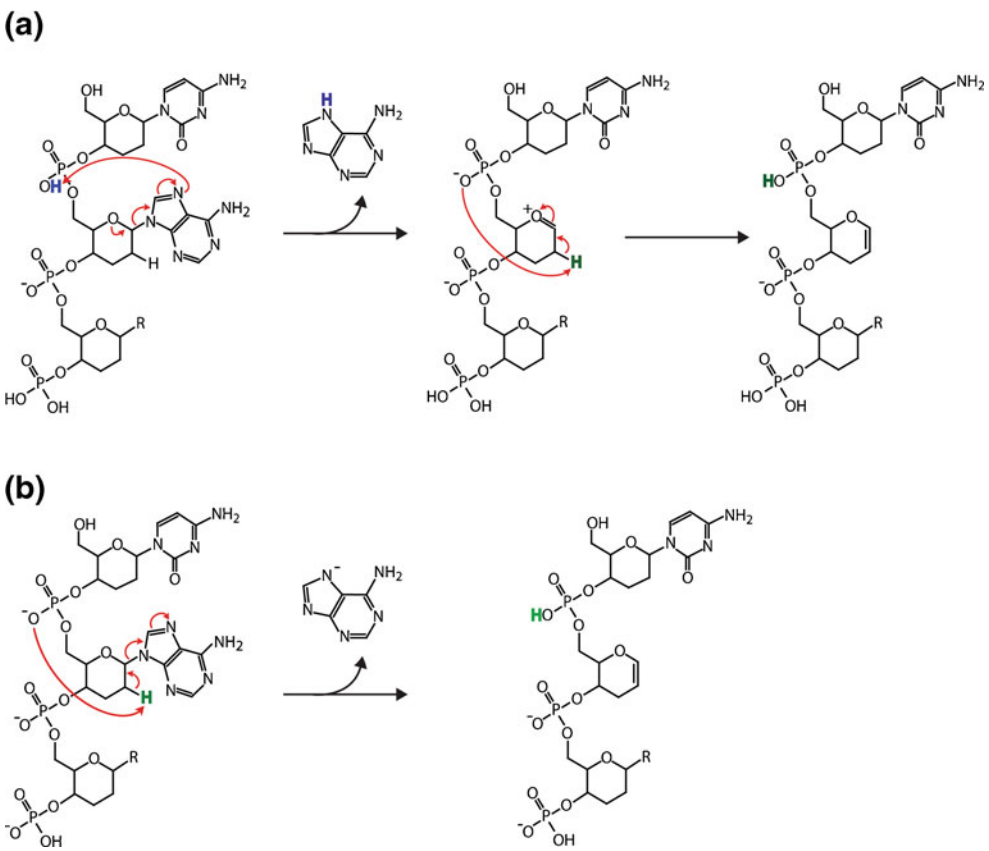

Scheme 2. Proposed mechanisms for the loss of a neutral **(a)** and a negatively charged nucleobase **(b)** from homo-DNA

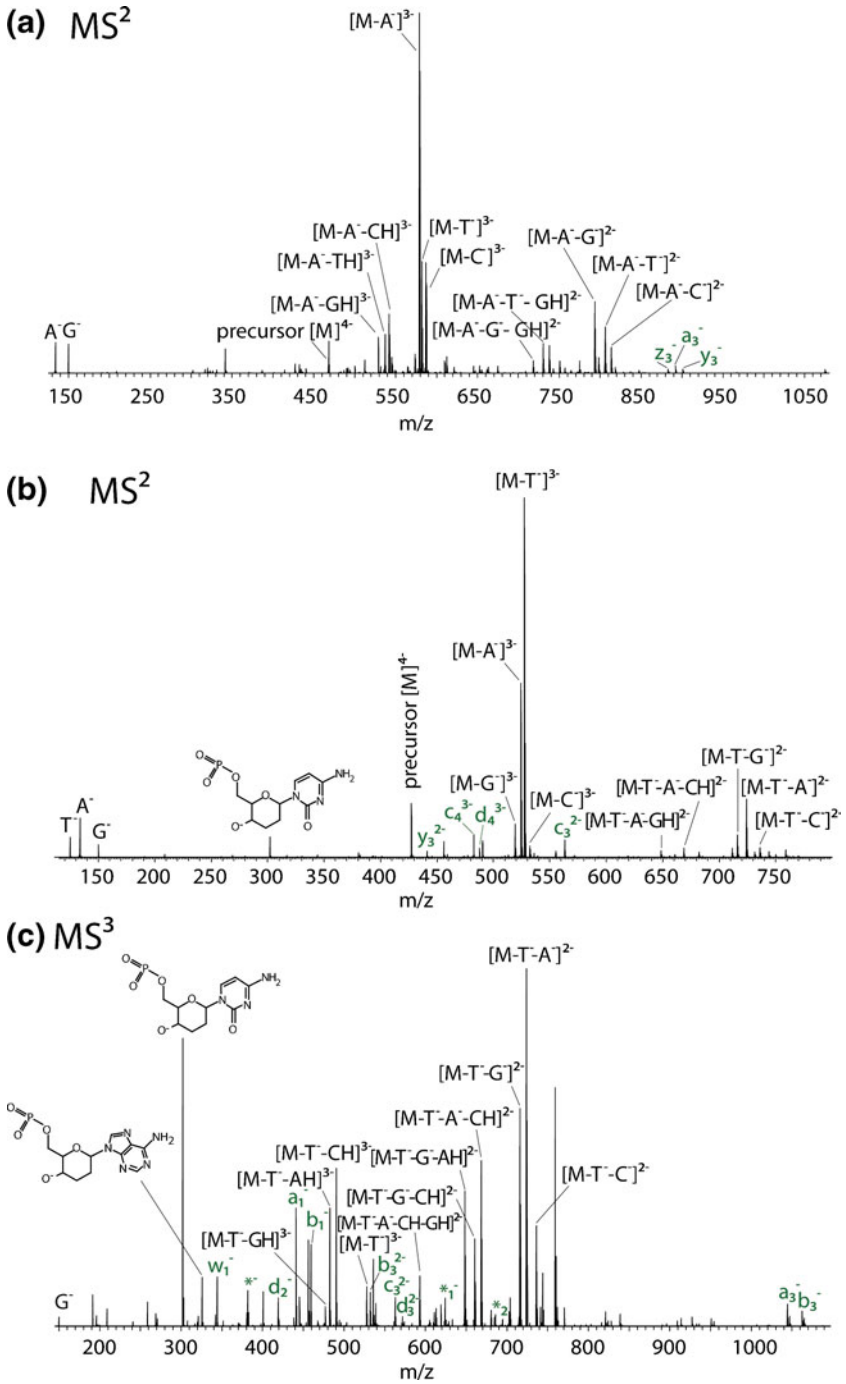

Figure 3. Product ion spectra obtained by ion trap CID of (**a**) the homo-DNA hexamer $(h(ACGTCG))^{4-}$ (*m/z* 467.852) and (**b**) the $(h(NH_2(CH_2)_6\text{-}GCCTA))^{4-}$ (*m/z* 426.854), demonstrating the strong tendency of homo-DNA for nucleobase loss. (**c**) MS^3 spectrum of $(h(NH_2(CH_2)_6\text{-}GCCTA) - T^-)^{3-}$ (*m/z* 527.459) providing sequence information due to formation of backbone fragments

neutral and negatively charged nucleobases, whereas fragment ions originating from backbone cleavage are of minor abundance only (Figure 1a). Considerably more information is obtained by CID of the corresponding DNA sequence, which results in extensive backbone dissociation and formation of the (a-B)- and w-ions (Figure 1b).

Nucleobase Loss

Precursor ions exhibiting reduced charge levels (ratio of the number of charges to the number of phosphate groups [33]) of less than approximately 40 % were found to undergo extensive loss of neutral nucleobases in the order of HG >

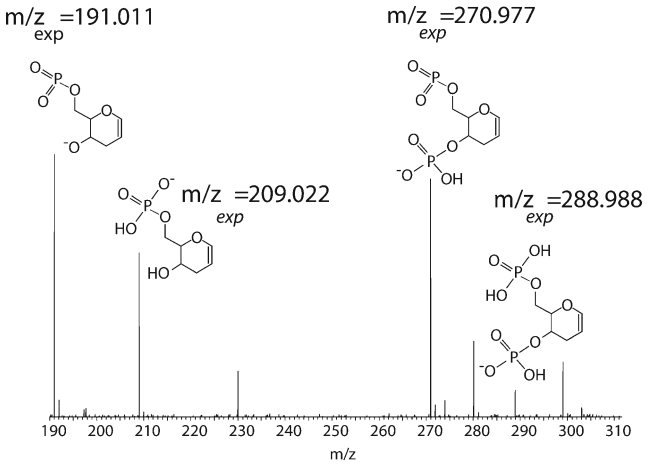

Figure 4. Section of the MS^3 spectrum of $(h(NH_2(CH_2)_6\text{-GCCTA}) - T^-)^{3-}$ (*m/z* 527.459), showing abundant peaks corresponding to hex-1-en pyranosyl backbone fragments

HA > HC ~ HT. This order agrees well with the reported order of the gas-phase proton affinities of the four nucleobases [34]. Nucleobase loss is influenced by the charge state of the precursor ion. Ion trap CID of the six-fold negatively charged 21-mer homo-DNA ***h1*** resulted in the simultaneous release of up to seven neutral nucleobases (Figure 1a), whereas at higher charge states, the loss of nucleobase anions becomes a more favorable pathway [35, 36]. This situation is reflected by the bar graphs in Figure 2, which show the base loss preferences for the two hexameric homo-DNA sequences ***h2*** and ***h3*** at different charge states. The doubly charged precursor ion shows the exclusive loss of neutral nucleobases, whereas for higher precursor charge states, the release of negatively charged nucleobases becomes the primary dissociation event. The loss of charged nucleobases is highly prominent in the case of quadruply charged homo-DNA hexamers (80 % charge level), which show the loss of nucleobase anions only.

Regarding the preferences for the release of charged nucleobases from highly charged homo-DNA hexamers, results are as controversial as the data reported on DNA in previous studies [34–36]. With increasing charge level ***h2*** and ***h3*** underwent preferential loss of negatively charged adenine, which is in agreement with Pan et al., who reported that the negative charge is more delocalized in adenine as it is for the other nucleobases [33]. However, significant differences between ***h2*** and ***h3*** were observed for the loss of charged guanine and the pyrimidine nucleobases, implying the presence of additional, so far unexplained, dynamics directing the loss of nucleobase anions.

For unmodified oligodeoxynucleotides, backbone cleavage and formation of [a-B]- and w-fragment ions is the inevitable consequence of neutral nucleobase loss. Gross and coworkers demonstrated that the scission of the 3'-C–O bond is the result of proton transfer reactions involving the 5'- and the 3'-phosphate groups, which sign responsible for the abstraction of the 4'- and 2'-proton, respectively [20]. In contrast to DNA, nucleobase loss from homo-DNA does not stringently lead to cleavage of the backbone. The six-membered pyranosyl ring of homo-DNA inhibits an electron rearrangement as in the case of DNA, thus preventing backbone cleavage. A potential mechanism for nucleobase loss from homo-DNA is depicted in Scheme 2. Since the preferences for neutral base loss were found to follow the order of the nucleobase's proton affinities, base protonation, most likely by the 6'-phosphate, must be the initial reaction step. After release of a nucleobase, stabilization of the ring structure is accomplished by abstraction of the 2'-proton attributable to reprotonation of the 6'-phosphate oxygen, and formation of a hex-1-en pyranose ring due to β-elimination (Scheme 2a). On the other hand, the release of a negatively charged nucleobase can be rationalized by direct attack of the 2'-proton by the already deprotonated 6'-phosphate group (Scheme 2b). In both cases, the structure of the remaining oligonucleotide is identical and cleavage of the backbone is not induced, even if multiple base losses take place, as demonstrated by the product ion spectrum of the 21-mer homo-DNA ***h1*** in Figure 1a. The products formed by nucleobase loss are well stabilized and even under the more stringent collision energy regime provided by higher-energy CID (HCD), no significantly increased formation of backbone fragments was observed (data not shown).

Backbone Dissociation

As demonstrated by the product ion spectra of ***h2*** and ***h4*** in Figure 3a and b, backbone dissociation products are of very low abundance and provide fragmentary sequence information only. The two spectra are characterized by the abundant peaks referring to the loss of neutral and charged nucleobases. In the low *m/z* range, the peaks of the released negatively charged nucleobases T^- (*m/z* 125.035), A^- (*m/z* 134.047), and G^- (*m/z* 150.042) are observed. Comparison of the two spectra reveals that the additional 6'-terminal phosphate group and hexylamine linker of ***h4*** do not affect the fragmentation of the oligonucleotide, thus excluding a charge-remote fragmentation mechanism. Figure 3b and c show the product ion spectra obtained by a MS^2 experiment on the pentanucleotide $(h[NH_2\{CH_2\}_6\text{-GCCTA}])^{4-}$ ***h4*** and MS^3 on its abundant $(h[NH_2\{CH_2\}_6\text{-GCCTA}] - T^-)^{3-}$ base loss fragment, respectively. Comparison of the two spectra demonstrates that further activation of $[M - B^-]^{n-}$ ions in MS^3 ion trap experiments is required to induce more comprehensive backbone cleavage. Due to the lack of a favored backbone dissociation channel, a balanced distribution of almost all possible types of fragment ions (a through d, and w through z) is generated. Thus, the gas-phase dissociation behavior of homo-DNA resembles the one of 2'-substituted ribose-based oligonucleotides, such as 2'-OMe [27] or 2'-F [21, 28], or LNA [29], which has been reported previously.

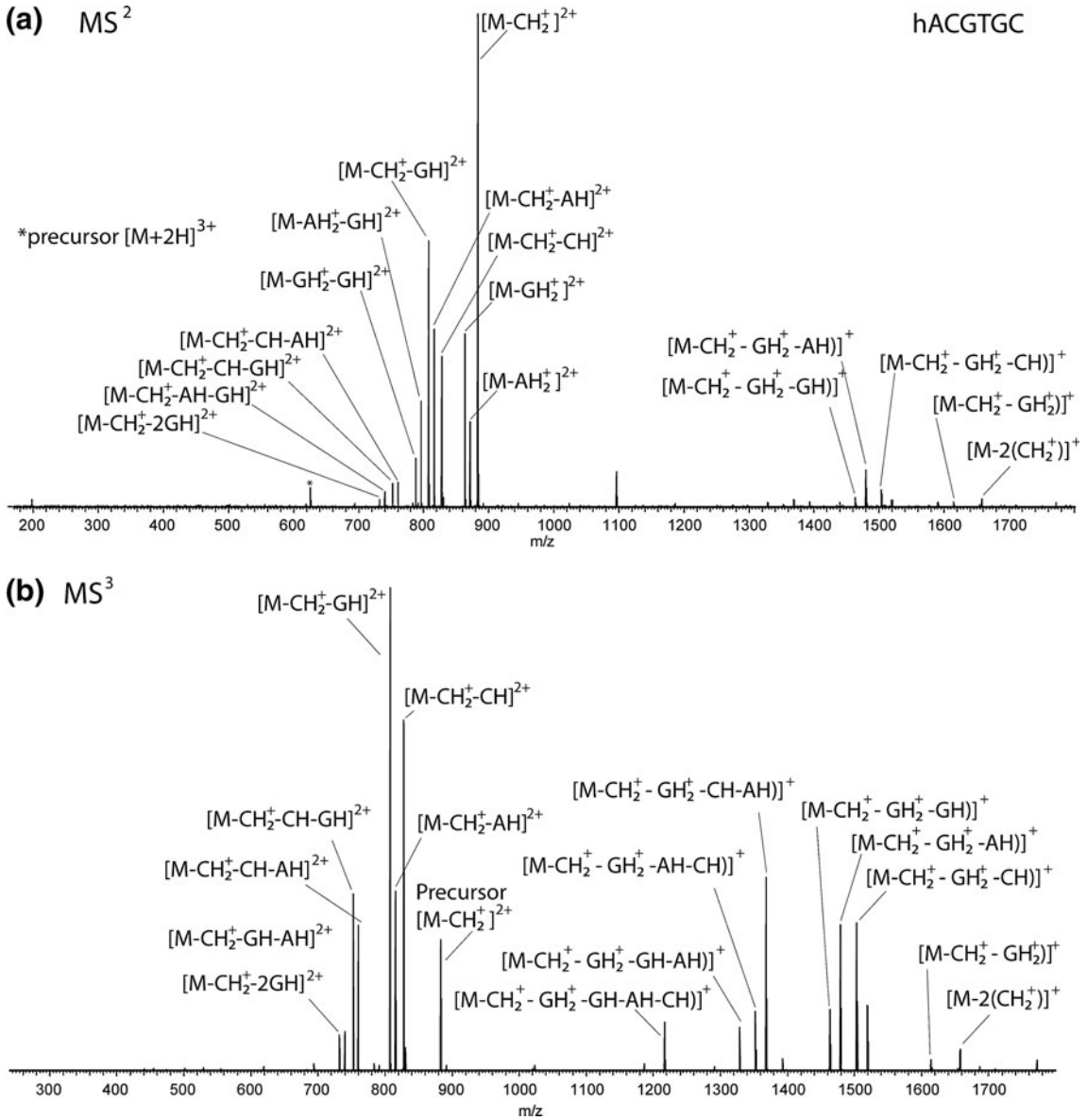

Figure 5. **(a)** Ion trap CID spectrum of the triply protonated sequence h(ACGTGC) **h2**. The spectrum gives evidence for the release of charged- and neutral nucleobases and multiple combinations thereof. Peaks related to backbone cleavage are hardly observed. **(b)** MS^3 spectrum of $[M - CH_2^+]^{2+}$. The second activation step results in even more pronounced nucleobase losses

The high degree of nucleobase loss from homo-DNA in combination with the unspecific backbone cleavage result in several short internal fragment ions not related to any specific type of nucleotide. The presence of these fragment ions supports the proposed base-loss mechanisms shown in Scheme 2. Peaks at *m/z* 191.011, *m/z* 209.022, *m/z* 270.977, and *m/z* 288.988 are indicative for the formation of the hex-1-en pyranosyl structure attributable to nucleobase loss during the first stage of collisional activation and repeated unspecific backbone cleavage in the second stage. The fragment ion structures, along with the MS^3 spectrum, are shown in Figure 4. The measured *m/z* ratios match the calculated values.

Collision-Induced Dissociation of homo-DNA Cations

Additionally, the homo-DNA sequences ***h1***–***h4*** were analyzed in the positive ion mode to complement the information extracted from the experiments performed in the negative ion mode. Generally, the overall dissociation behavior of homo-DNA cations resembles the one of the anions, with multiple loss of neutral and positively charged nucleobases being the predominant fragmentation pathway upon CID. As a representative example, the product ion spectrum obtained by ion trap CID of the triply protonated homo-DNA hexamer ***h2*** (*m/z* 626.153) is shown in

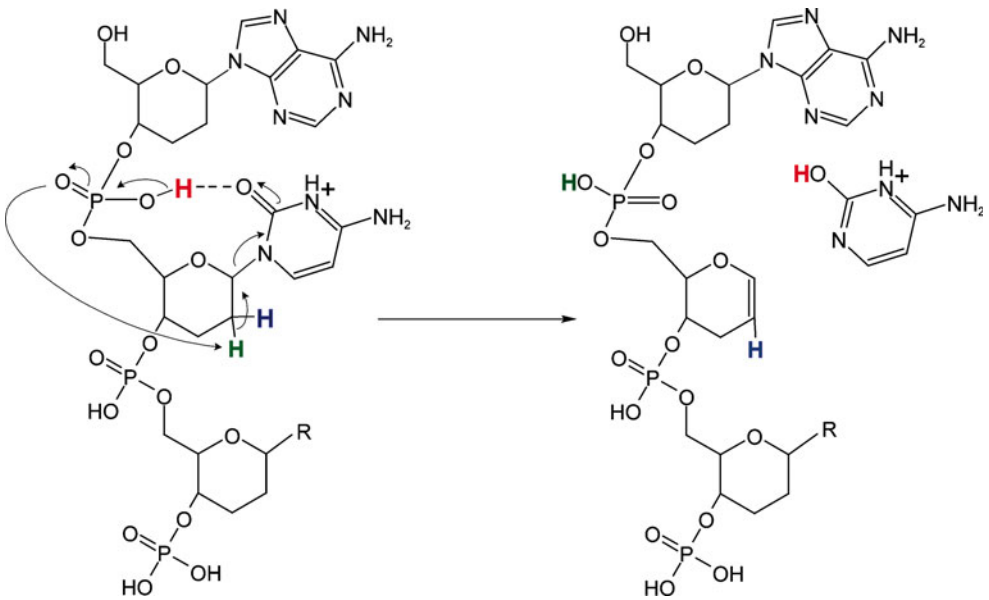

Scheme 3. Proposed mechanism for release of a charged nucleobase from protonated homo-DNA

Figure 5a. The release of positively charged cytosine is preferred over GH_2^+ and AH_2^+, and the loss of TH_2^+ is suppressed completely. These findings are in good agreement with the order of nucleobase loss observed for protonated trimeric oligodeoxynucleotides [37] and can be rationalized by the relative proton affinities of the corresponding bases [34]. Also, a very limited number of sequence-defining ions is generated by the MS^3 experiments (Figure 5b).

Scheme 3 shows the proposed mechanism for the release of positively charged nucleobases from homo-DNA cations. Oligonucleotide cations exhibit a neutral phosphate backbone and the positive charges are assumed to reside at the

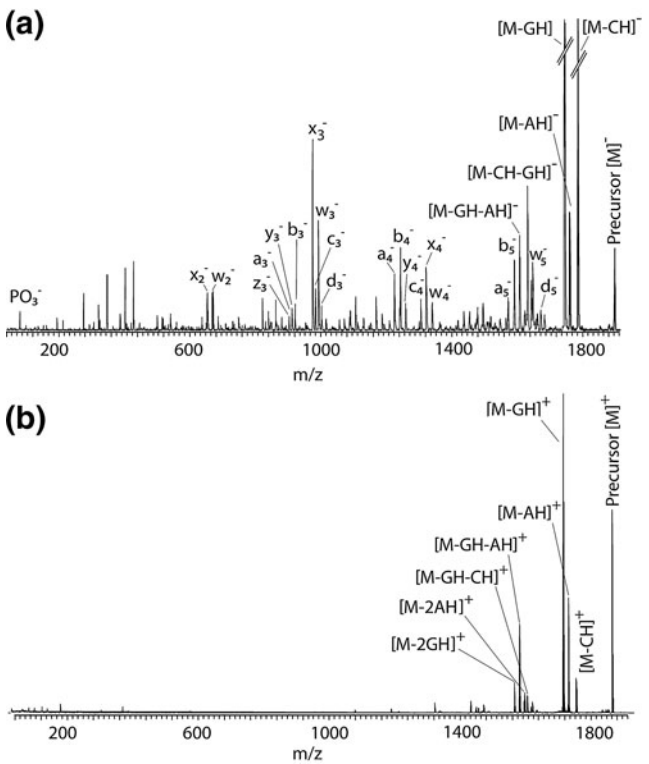

Figure 6. MALDI-LIFT-MS/MS spectra of h(ACGTGC) (**h2**) in the **(a)** negative ion mode and **(b)** the positive ion mode giving evidence for single and double nucleobase loss from the precursor, unspecific backbone dissociation, and the formation of nucleobase-independent internal fragment ions; (*internal fragments)

nucleobases. The formation of a hydrogen bond between the nucleobase (the cytosine C-2 oxygen in the example shown) and the 5'-phosphate group facilitates proton transfer to the nucleobase and initiates abstraction of the 2'-proton by the phosphate group, which eventually results in scission of the weakened *N*-glycosidic bond and release of the positively charged nucleobase as a result of the β-elimination at the 1'- and 2'-carbon atoms of the hexopyranosyl sugar moiety. Such reaction cascade has been proposed previously by Andersen et al. for nucleobase loss from protonated RNA [24]. Release of a positively charged nucleobase from protonated DNA has been demonstrated by Vrkic et al. [37] to result in backbone dissociation. However, in the case of homo-DNA, with the sugar ring expanded by an additional methylene group, the product is a well-stabilized hex-1-en pyranosyl structure (Scheme 3), which halts the reaction cascade and prevents subsequent backbone cleavage.

Metastable Decay of MALDI-Generated homo-DNA Anions and Cations

MALDI-MS/MS experiments on singly negatively charged *homo*-DNA led to comparable results, as demonstrated by the LIFT-MALDI-MS/MS spectrum [32] of the sequence ***h2*** in Figure 6a. The observed product ion pattern strongly resembles the one obtained by negative mode ESI-MS/MS. The loss of neutral nucleobases is the predominant fragmentation pathway and follows the order of GH > CH > AH >>> TH. Though weak, all series of sequence-defining fragment ions are present in the spectrum, and signal of internal fragment ions is observed in the low mass range. Despite the fact that loss of neutral nucleobases is the dominating event for precursors of both polarities, hardly any peaks corresponding to backbone dissociation products are found in the spectra of singly, positively charged precursors (Figure 6b). These observations support the above-described formation of stable primary fragments as a result of nucleobase loss. In the case of a positively charged precursor ion, the lack of a negatively charged phosphate group impedes significant backbone cleavage, suggesting that the availability of such a group is crucial for backbone dissociation of homo-DNA.

Conclusions

Regarding the continuing focus on highly modified oligonucleotide analogues for therapeutic and diagnostic purposes, optimized analytical tools are needed for structure validation. Compared with naturally occurring nucleic acids, the hexopyranosyl-based homo-DNA exhibits a considerably different gas-phase dissociation behavior. The enlarged sugar ring structure decouples nucleobase loss from backbone dissociation, thus resulting in stable primary fragment ions. The generation of sequence-defining backbone fragments requires at least one additional stage of ion activation (MS^3). Backbone dissociation of homo-DNA is characterized by unspecific cleavage of the internucleoside phosphate linkers, resulting in a balanced distribution of all the possible fragment ion series. This study provide fundamental information about the gas-phase dissociation of bioorthogonal homo-DNA and, furthermore, reveal some detail of the gas-phase dissociation mechanism of negatively charged DNA, which has been proposed 15 years ago by Wang et al. [20]. In this mechanism, a zwitterionic intermediate is formed by nucleobase loss and undergoes double β-elimination to cleave the 3'-C–O bond and form the furan structure of the 5'-terminal (a-B)-fragment ion. However, literature does not provide any rationale whether this second step of DNA dissociation is initiated by abstraction of the 2'-proton, the 4'-proton, or proceeds as a concerted reaction. If we apply the findings of our investigation of homo-DNA to the dissociation of DNA, we have to conclude that the abstraction of the 2'-proton must be the initial event in the dissociation of the zwitterionic intermediate. The abstraction of the ribose 4'-proton in DNA corresponds to abstraction of the hexopyranose 5'-proton in homo-DNA and would stringently result in backbone cleavage of homo-DNA, which was not observed.

Acknowledgments

The authors gratefully acknowledge financial support of this work by the Swiss National Science Foundation (grant no. 200020_140628/1).

References

1. Dias, N., Stein, C.A.: Antisense oligonucleotides: basic concepts and mechanisms. Mol. Cancer Ther. **1**, 347–355 (2002)
2. Saonere, J.A.: Antisense therapy, a magic bullet for the treatment of various diseases: present and future prospects. J. Med. Genet. Genom. **3**, 77–83 (2011)
3. Singh, J., Kaur, H., Kaushik, A., Peer, S.: A review of antisense therapeutic interventions for molecular biological targets in various diseases. Int. J. Pharmacol. **7**, 294–315 (2011)
4. Leumann, C.J.: DNA analogues: from supramolecular principles to biological properties. Bioorg. Med. Chem. **10**, 841–854 (2002)
5. Deleavey, G.F., Damha, M.J.: Designing chemically modified oligonucleotides for targeted gene silencing. Chem. Biol. **19**, 937–954 (2012)
6. Shibata, A., Abe, H., Ito, Y.: Oligonucleotide-templated reactions for sensing nucleic acids. Molecules **17**, 2446–2463 (2012)
7. Jentzsch, E., Mokhir, A.: A fluorogenic, nucleic acid directed "click" reaction. Inorg. Chem. **48**, 9593–9595 (2009)
8. Franzini, R.M., Kool, E.T.: Efficient nucleic acid detection by template reductive quencher release. J. Am. Chem. Soc. **131**, 16021–16023 (2009)
9. Erben, A., Grossmann, T.N., Seitz, O.: DNA-instructed acyl transfer reactions for the synthesis of bioactive peptides. Bioorg. Med. Chem. Lett. **21**, 4993–4997 (2011)
10. Ma, Z.C., Taylor, J.S.: Nucleic acid-triggered catalytic drug release. Proc. Natl. Acad. Sci. U. S. A. **97**, 11159–11163 (2000)
11. Okamoto, A., Tanabe, K., Inasaki, T., Saito, I.: Phototriggered drug release from functionalized oligonucleotides by a molecular beacon strategy. Angew. Chem. Int. Ed. **42**, 2502–2504 (2003)
12. Stoop, M., Désiron, C., Leumann, C.J.: Nucleic acid sensing by an orthogonal reporter system based on homo-DNA. Artificial DNA: PNA & XNA **4**, 28–33 (2013)
13. Eschenmoser, A.: Chemical etiology of nucleic acid structure. Science **284**, 2118–2124 (1999)
14. Egli, M., Lubini, P., Pallan, P.S.: The long and winding road to the structure of homo-DNA. Chem. Soc. Rev. **36**, 31–45 (2007)

15. Egli, M., Pallen, P.S., Prattanayek, R., Wilds, C.J., Lubini, P., Minasov, G., Dobler, M., Leumann, C.J., Eschenmoser, A.: Crystal structure of homo-DNA and nature's choice of pentose over hexose in the genetic system. J. Am. Chem. Soc. **128**, 10847–10856 (2006)
16. Leumann, C.J.: Sugar modification as a means to increase the biological performance of oligonucleotides. Nucleic Acids Res. Symp. Ser. **50**, 55–56 (2006)
17. Crey-Desbiolles, C., Ahn, D.R., Leumann, C.J.: Molecular beacons with a homo-DNA stem: improving target selectivity. Nucleic Acids Res. **33**, e77 (2005)
18. Stoop, M., Leumann, C.J.: Homo-DNA templated chemistry and its application to nucleic acid sensing. Chem. Commun. **47**, 7494–7496 (2011)
19. McLuckey, S.A., Van Berkel, G.J., Glish, G.L.: Tandem mass spectrometry of small, multiply charged oligonucleotides. J. Am. Soc. Mass Spectrom. **3**, 60–70 (1992)
20. Wang, Z., Wan, X., Ramanathan, R., Taylor, J.S., Gross, M.J.: Structure and fragmentation mechanisms of isomeric T-rich oligonucleotides: a comparison of four tandem mass spectrometric methods. J. Am. Soc. Mass Spectrom. **9**, 683–691 (1998)
21. Tromp, J.M., Schürch, S.: Gas-phase dissociation of oligoribonucleotides and their analogs studied by electrospray ionization tandem mass spectrometry. J. Am. Soc. Mass Spectrom. **16**, 1262–1268 (2005)
22. Huang, T.-Y., Kharlamova, A., Liu, J., McLuckey, S.A.: Ion trap collision-induced dissociation of multiply deprotonated RNA: c/y-ions versus (a-B)/w-ions. J. Am. Soc. Mass Spectrom. **19**, 1832–1840 (2008)
23. Gross, J., Leisner, A., Hillenkamp, F., Hahner, S., Karas, M., Schäfer, J., Lützenkirchen, F., Nordhoff, E.: Investigations of the metastable decay of DNA under ultraviolet matrix-assisted laser desorption/ ionization conditions with post-source-decay analysis and hydrogen/ deuterium exchange. J. Am. Soc. Mass Spectrom. **9**, 866–878 (1998)
24. Andersen, T.E., Kirpekar, F., Haselmann, K.F.: RNA fragmentation in MALDI mass spectrometry studied by H/D-exchange: mechanisms of general applicability to nucleic acids. J. Am. Soc. Mass Spectrom. **10**, 1353–1368 (2006)
25. Wu, J., McLuckey, S.A.: Gas-phase fragmentation of oligonucleotide ions. Int. J. Mass Spectrom. **237**, 197–241 (2004)
26. Wan, K.X., Gross, M.L.: Fragmentation mechanisms of oligodeoxynucleotides: effects of replacing phosphates with methylphosphonates and thymines with other bases in T-rich sequences. J. Am. Soc. Mass Spectrom. **12**, 580–589 (2000)
27. Nyakas, A., Stucki, S.R., Schürch, S.: Tandem mass spectrometry of modified and platinated oligoribonucleotides. J. Am. Soc. Mass Spectrom. **22**, 875–887 (2011)
28. Gao, Y., McLuckey, S.A.: Collision-induced dissociation of oligonucleotide anions fully modified at the 2'-position of the ribose: 2'-F/-H and 2'-F/-H/-OMe mix-mers. J. Mass Spectrom. **47**, 364–369 (2012)
29. Huang, T.-Y., Kharlamova, A., McLuckey, S.A.: Ion trap collision-induced dissociation of locked nucleic acids. J. Am. Soc. Mass Spectrom. **21**, 144–153 (2010)
30. Böhringer, M., Roth, H.-J., Hunziker, J., Göbel, M., Krishnan, R., Giger, A., Schweizer, B., Schreiber, J., Leumann, C.J., Eschenmoser, A.: Warum Pentose- und nicht Hexose-Nucleinsäuren? Teil II. Oligonucleotide aus 2',3'-Dideoxy-beta-D-glucopyranosyl-Bausteinen ("Homo-DNS"): Herstellung. Helv. Chim. Acta **75**, 1416–1477 (1992)
31. Nyakas, A., Blum, L.C., Stucki, S.R., Reymond, J.-L., Schürch, S.: OMA and OPA— software-supported mass spectra analysis of native and modified nucleic acids. J. Am. Soc. Mass Spectrom. **24**, 249–256 (2013)
32. Suckau, D., Resemann, A., Schuerenber, M., Hufnagel, P., Franzen, J., Holle, A.: A novel MALDI LIFT-TOF/TOF mass spectrometer for proteomics. Anal. Bioanal. Chem. **367**, 952–956 (2003)
33. Pan, S., Verhoevern, K., Lee, J.K.: Investigation of the initial fragmentation of oligodeoxynucleotides in a quadrupole ion trap: charge level-related base loss. J. Am. Soc. Mass Spectrom. **16**, 1853–1865 (2005)
34. Liguori, A., Napoli, A., Sindona, G.: Survey of the proton affinities of adenine, cytosine, thymine and uracil dideoxyribonucleotides, deoxyribonucleotides, and ribonucleotides. J. Mass Spectrom. **35**, 139–144 (2000)
35. McLuckey, S.A., Vaidyanathan, G., Habibi-Goudarzi, S.: Charged versus neutral nucleobase loss from multiply charged. J. Mass Spectrom. **30**, 1222–1229 (1995)
36. Daneshfar, R., Klassen, J.S.: Thermal decomposition of multiply charged T-rich oligonucleotide anions in the gas phase. Influence of internal solvation on the Arrhenius parameters for neutral nucleobase loss. J. Am. Soc. Mass Spectrom. **17**, 1229–1238 (2006)
37. Vrkic, A.K., O'Hair, R.A.J., Foote, S., Reid, G.E.: Fragmentation reactions of all 64 protonated trimer oligodeoxynucleotides and 16 mixed base tetramer oligodeoxynucleotides via tandem mass spectrometry in an ion trap. Int. J. Mass Spectrom. **194**, 145–164 (2000)